

External luminescence and photon recycling in near-field thermophotovoltaics

John DeSutter^{*}, Rodolphe Vaillon^{**, *} and Mathieu Francoeur^{*,†}

^{*}*Radiative Energy Transfer Lab, Department of Mechanical Engineering, University of Utah, Salt Lake City, UT 84112, USA*

^{**}*Univ Lyon, CNRS, INSA-Lyon, Université Claude Bernard Lyon 1, CETHIL UMR5008, F-69621, Villeurbanne, France*

ABSTRACT

The importance of considering near-field effects on photon recycling and spontaneous emission in a thermophotovoltaic device is investigated. Fluctuational electrodynamics is used to calculate external luminescence from a photovoltaic cell as a function of emitter type, vacuum gap thickness between emitter and cell, and cell thickness. The observed changes in external luminescence suggest strong modifications of photon recycling caused by the presence of the emitter. Photon recycling for propagating modes is affected by reflection at the vacuum-emitter interface and is substantially decreased by the leakage towards the emitter through tunneling of frustrated modes. In addition, spontaneous emission by the cell can be strongly enhanced by the presence of an emitter supporting surface polariton modes. It follows that using a radiative recombination model with a spatially uniform radiative lifetime, even corrected by a photon recycling factor, is inappropriate. Applying the principles of detailed balance, and accounting for non-radiative recombination mechanisms, the impact of external luminescence enhancement in the near field on thermophotovoltaic performance is investigated. It is shown that unlike isolated

[†] Corresponding author. Tel.: +1 801 581 5721
Email address: mfrancoeur@mech.utah.edu

cells, the external luminescence efficiency is not solely dependent on cell quality, but significantly increases as the vacuum gap thickness decreases below 400 nm for the case of an intrinsic silicon emitter. In turn, the open-circuit voltage and power density benefit from this enhanced external luminescence toward the emitter. This benefit is larger as cell quality, characterized by the contribution of non-radiative recombination, decreases.

I. INTRODUCTION

A thermophotovoltaic (TPV) device converts thermal energy into electricity and consists primarily of an emitter and a photovoltaic (PV) cell separated by a vacuum gap [1,2]. The emitter is heated by an external source such as the sun [3,4] or a residential boiler [5] among others and, in turn, emits thermal radiation which is used to generate electron-hole pairs (EHPs) within the PV cell. TPV devices hold great potential for both solar-to-electrical energy conversion and waste heat recovery, and are expected to be quiet, modular, safe and pollution free [1].

TPV performance can be potentially enhanced when the vacuum gap separating the emitter and cell is decreased to less than the thermal wavelength λ_T . At a sub-wavelength gap thickness, thermal radiation is in the near-field regime such that heat transfer can exceed the blackbody limit. This is due to the contribution of evanescent modes, decaying exponentially within a distance of approximately a wavelength normal to the surface of a heat source, which accompany the propagating modes described by Planck's theory [6-16]. These evanescent modes can be generated by total internal reflection at an interface (frustrated modes) and through phonon or free electron oscillations (surface polariton modes). In a TPV system, it is expected that the contribution of evanescent modes leading to an increase of photon absorption, and thus an increase of the generation rate of EHPs in the cell, results in enhanced device performance [17-33].

In addition to the enhancement of photon absorption in the near field, there is also an increase in photon emission from the cell lost to the surroundings, or external luminescence. This enhancement can be caused by a drop in the reabsorption of internally emitted photons, called photon recycling, due to tunneling of frustrated modes from the cell to the emitter, and by an

increase in the cell internal spontaneous emission rate due to surface polariton modes supported by the emitter [20,34]. Using the principles of detailed balance [35], these mechanisms can be accounted for by directly relating radiative recombination to the external luminescence from the cell [23-25,29,31].

A different approach commonly used to model radiative recombination in near-field TPVs involves a radiative lifetime in which only spontaneous photon emission, or internal luminescence, in the cell is considered [20,22,26,28,30,32]. It has been shown that with this approach, photon recycling is neglected [36]. To circumvent this, the radiative lifetime is sometimes corrected using a photon recycling factor, but near-field impacts on photon recycling are still unaccounted for in this approach. Modeling radiative recombination via a radiative lifetime also neglects potential near-field impacts on the internal spontaneous emission within cell. Laroche et al. [20] concluded that the impact of surface polariton modes on radiative lifetime is negligible, since it only affects a very small portion of the cell. However, photon recycling was not accounted for in their analysis.

In this work, near-field impacts on radiative recombination in TPV devices are investigated when photon recycling and spontaneous emission effects are simultaneously accounted for. This is accomplished by analyzing the different photon modes contributing to the cell near-field external luminescence calculated via fluctuational electrodynamics. The impacts on external luminescence of the presence of the emitter, emitter type, vacuum gap thickness and cell thickness are investigated. Internal and external luminescence of an isolated cell, i.e. with no emitter, are used to evaluate the modification in photon recycling caused by the presence of the emitter. In addition, the impact of enhanced external luminescence on near-field TPV performance is analyzed when including non-radiative recombination mechanisms.

II. DESCRIPTION OF THE PROBLEM

The near-field TPV device outlined in Fig. 1 is considered, in which a semi-infinite bulk emitter and a PV cell with thickness t are separated by a vacuum gap of thickness d . The emitter and the cell are at constant and uniform temperatures of $T_e = 800$ K and $T_c = 300$ K. The cell consists of gallium antimonide (GaSb) and has a bandgap energy of $E_g = 0.72$ eV (bandgap frequency of $\omega_g = 1.09 \times 10^{15}$ rad/s) at 300 K [37]. For frequencies above ω_g , the interband dielectric function of GaSb is calculated via the model provided in Ref. [38] and is assumed to be independent of dopant level and type. In this frequency band, the lattice and free carriers contribution to the dielectric function is negligible [22]. The cell substrate is modeled as a semi-infinite layer with a frequency independent dielectric function of $\epsilon_s = 1 + i\delta$ where $\delta \rightarrow 0$. This generalization is made for simplicity, but does not compromise the main conclusions of the analysis. Two types of emitters are considered: an emitter made of intrinsic silicon (Si) where the dielectric function is taken from Ref. [39] and an emitter made of a material supporting surface polariton modes. The dielectric function of the material supporting surface polariton modes is described by a Drude model $\epsilon_{Dr} = 1 - \omega_p^2 / (\omega^2 + i\omega\Gamma)$, where ω_p is the plasma frequency and Γ is the loss coefficient [40]. The values of ω_p and Γ are fixed at 1.83×10^{15} rad/s and 2.10×10^{13} rad/s, respectively [26]. The device is assumed to be azimuthally symmetric and infinite in the ρ -direction making the view factor unity between the emitter and the cell. This implies that only variations of absorption and emission in the z -direction are of concern. The cell is discretized strictly along z into N discrete layers of equal thickness Δz_j .

The available photon modes contributing to external luminescence from the cell can be described in terms of the parallel wavevector k_ρ [rad/m] (Fig. 1). Propagating modes in the cell are

characterized by parallel wavevectors $0 < k_\rho < \text{Re}(m_c)k_0$, where m_c is the refractive index of the cell and $k_0 = \omega/c_0$ is the vacuum wavevector. To better understand how the presence of the emitter impacts the available photon modes contributing to external luminescence, an isolated cell surrounded by vacuum is first considered. In this case, only propagating modes in vacuum with $0 < k_\rho < k_0$ can escape the cell and contribute to external luminescence. These photon modes can be partially recycled, a phenomenon through which a photon generated via EHP recombination is reabsorbed by the cell and generates an additional EHP [36]. Here, photon recycling includes partial reabsorption of internally emitted modes along their pathlength. Photon modes with $k_0 < k_\rho < \text{Re}(m_c)k_0$ cannot escape the cell due to total internal reflection at the boundaries and, therefore, are all recycled.

In a TPV device where the emitter is in the far field of the cell ($d \gg \lambda_T$), external luminescence is gap-independent and is limited to propagating modes in vacuum. In addition to the mechanisms outlined above for the isolated cell, photon recycling can occur via reabsorption by the cell of modes reflected at the vacuum-emitter interface.

In a TPV device where the emitter and the cell are separated by a sub-wavelength gap ($d < \lambda_T$), external luminescence is gap-dependent due to interference of propagating modes and tunneling of evanescent modes from the cell to the emitter. Propagating modes in the cell experiencing total internal reflection generate frustrated modes with decaying evanescent fields in vacuum. Tunneling of these frustrated modes from the cell to the emitter increases the available photon modes that can escape the cell beyond the vacuum limit of k_0 , thus decreasing the number of recycled photons compared to the far-field case. If, instead, a Drude emitter supporting surface polariton modes is used, the available k_ρ modes can be further increased beyond the propagating

limit in the cell, $\text{Re}(m_c)k_0$, as their presence can greatly modify the local density of photon modes in the cell [34], impacting spontaneous emission.

The near-field external luminescence of the GaSb cell in the presence of the Si and Drude emitters is analyzed next.

III. NEAR-FIELD EXTERNAL LUMINESCENCE

The current density J [A/cm^2] in the cell can be described by the difference between the rate of above bandgap photon absorption per unit area γ_a [$(\text{photons})/(\text{cm}^2\text{s})$] and the rate of above bandgap photon emission lost to the surroundings per unit area, also called external luminescence, γ_e [$(\text{photons})/(\text{cm}^2\text{s})$] [35]:

$$J(d, V) = q[\gamma_a(d) - \gamma_e(d, V)] \quad (1)$$

where V [V] is the applied voltage of an external load and q [1.6022×10^{-19} C] is the electron charge. The distinction of emission lost to the surroundings is made as in the presence of an emitter, some of the cell emission can be reflected at the vacuum-emitter interface and reabsorbed by the cell, thus contributing to photon recycling. Equation (1) is valid assuming that there is only radiative recombination (radiative limit), every above bandgap photon absorbed by the cell generates one EHP, every EHP that recombines produces one photon and charge carriers have infinite mobility allowing for all generated electrons and holes to be collected [35,36,41]. The main benefit of near-field TPVs is the enhancement of photon absorption γ_a due to tunneling of evanescent modes from the emitter to the cell.

To account for all photon modes described in Section II, the fluctuational electrodynamics formalism is used. It involves the addition to Maxwell's equations of a thermally induced

fluctuating current density representing thermal emission [42]. The link between the local temperature of a heat source and the fluctuating current density is provided by the fluctuation-dissipation theorem [42]. Fluctuational electrodynamics is applicable for gap thicknesses in both the far and near field, and its validity has been confirmed experimentally [43] and theoretically [44] down to separation gaps of 2 nm and 1 nm, respectively. Using this formalism, the above bandgap photon flux absorbed by the cell is calculated by summing the rate of photons absorbed within a discrete layer Δz_j over all N layers [29]:

$$\gamma_a(d) = \sum_{j=1}^N \int_{\omega_g}^{\infty} \frac{1}{\hbar\omega} \Theta(\omega, T_e, 0) \Phi_{e-c}(\omega, d, \Delta z_j) d\omega \quad (2)$$

where Θ is the mean energy of a generalized Planck oscillator defined as [29,45]:

$$\Theta(\omega, T, V) = \frac{\hbar\omega}{\exp[(\hbar\omega - qV)/k_b T] - 1} \quad (3)$$

The term Φ_{e-c} is the spectral, gap-dependent transmission factor relating the emitter to a discrete layer Δz_j within the cell. The transmission factor, provided in the Appendix, is calculated from dyadic Green's functions and accounts for all modes, propagating and evanescent [46].

External luminescence, which accounts for emission lost toward the emitter ($\gamma_{e,c-e}$) and the substrate ($\gamma_{e,c-s}$), is given by:

$$\gamma_e(d, V) = \sum_{j=1}^N \int_{\omega_g}^{\infty} \frac{1}{\hbar\omega} \Theta(\omega, T_c, V) [\Phi_{c-e}(\omega, d, \Delta z_j) + \Phi_{c-s}(\omega, d, \Delta z_j)] d\omega \quad (4)$$

where Φ_{c-e} and Φ_{c-s} are the spectral, gap-dependent transmission factors relating a discrete layer Δz_j within the cell to the emitter and substrate, respectively. The transmission factor Φ_{c-e} is the same as Φ_{e-c} due to the reciprocity of the dyadic Green's functions [22]. The transmission factor Φ_{c-s} is provided in the Appendix. Equation (4) is valid for non-degenerate conditions and when the charge carriers have infinite mobility thus allowing for uniform quasi-Fermi level splitting throughout the cell which can be described by the applied voltage as qV [36,41].

Under the Boltzmann approximation, which is appropriate when $(E_g - qV) \gg k_b T_c$ [41,47] and when E_g is larger than 0.5 eV [47], external luminescence can be expressed as [36]:

$$\gamma_e(d, V) = \gamma_e^0(d) \exp\left[\frac{qV}{k_b T_c}\right] \quad (5)$$

In Eq. (5), the contribution in chemical equilibrium ($V = 0$) to external luminescence γ_e^0 [(photons)/(cm²s)] is:

$$\gamma_e^0(d) = \sum_{j=1}^N \int_{\omega_g}^{\infty} \frac{1}{\exp[\hbar\omega / k_b T_c]} [\Phi_{c-e}(\omega, d, \Delta z_j) + \Phi_{c-s}(\omega, d, \Delta z_j)] d\omega \quad (6)$$

Figure 2 shows the cell external luminescence in chemical equilibrium per unit angular frequency and parallel wavevector, γ_{e,ω,k_p}^0 , for the Si and Drude emitters when the gap and cell thicknesses are fixed at $d = 10$ nm and $t = 10$ μm . In the presence of the Si emitter, frustrated modes described by normalized parallel wavevectors $1 < k_p/k_0 < \min[\text{Re}(m_{Si}), \text{Re}(m_c)]$, where m_{Si} is the refractive index of Si, contribute significantly to the cell near-field external luminescence. For the case of the GaSb cell, the upper k_p/k_0 limit is $\text{Re}(m_{Si})$ for all frequencies of interest. Note

that $\text{Re}(m_{Si}) = 3.46$ at the bandgap frequency ω_g of GaSb, and is nearly constant in the ω -band shown in Fig. 2(a). This implies that the presence of a Si emitter in the near field of the cell opens a new channel for external luminescence since modes with $1 < k_\rho/k_0 < \text{Re}(m_{Si})$, fully contributing to photon recycling in far-field TPVs, can now escape the cell. This has the effect of decreasing photon recycling and, consequently, increasing the impact of radiative recombination. Modes with $\text{Re}(m_{Si}) < k_\rho/k_0 < \text{Re}(m_c)$ cannot propagate in Si and, therefore, cannot be tunneled from the cell to the emitter and are thus completely recycled. External luminescence towards the substrate, occurring through modes described by $0 < k_\rho/k_0 < 1$, remains unchanged causing the sudden transition at $k_\rho/k_0 = 1$.

The photon mode limit established for the Si emitter is not appropriate when the emitter supports surface polariton modes. This is the case for the Drude emitter in which there is a significant enhancement in the available photon modes beyond the cell propagating limit of $k_\rho/k_0 = \text{Re}(m_c)$ contributing to external luminescence (Fig. 2b). This is because the local density of photon modes in the cell is greatly modified by the presence of the Drude emitter when $d < \lambda_T$ [34]. At the frequencies where the Drude emitter supports surface polaritons, the limiting mode contributing to external luminescence is gap-dependent and can be approximated by $k_\rho \approx 1/d$ [48,49] which leads to a value of $k_\rho/k_0 \approx 27$. This is in reasonable agreement with the results in Fig. 2(b). Therefore, an emitter supporting surface polariton modes opens an additional channel for external luminescence. Here, since the Drude emitter supports surface polaritons at frequencies for which emission by the cell is significant, this leads to a large enhancement of the cell external luminescence.

In Fig. 3, external luminescence in chemical equilibrium, γ_e^0 , is shown as a function of vacuum gap thickness d for the Si and Drude emitters when the cell thickness is fixed at 10 μm . In order to quantify the modification of photon recycling due to the presence of the emitter, internal luminescence can be used as a reference. Volumetric internal luminescence within an isolated PV cell in chemical equilibrium is quantified by the rate of above bandgap spontaneous photon emission per unit volume $\bar{\gamma}_{i,ic}^0$ [(photons)/(cm^3s)] [50,51]:

$$\bar{\gamma}_{i,ic}^0 = \frac{1}{\pi^2 c_0^2} \int_{\omega_g}^{\infty} (\text{Re}(m_c))^2 \alpha_c \frac{\omega^2}{\exp[\hbar\omega/k_b T_c] - 1} d\omega \quad (7)$$

where α_c [cm^{-1}] is the frequency-dependent absorption coefficient of the cell calculated using the dielectric function of GaSb. Under the Boltzmann approximation, the minus one term in the denominator of Eq. (7) can be removed such that under a bias V , the rate of spontaneous photon emission cumulated over the cell is given by [45,51]:

$$\gamma_{i,ic}(V) = \bar{\gamma}_{i,ic}^0 \exp\left[\frac{qV}{k_b T_c}\right] \quad (8)$$

where $\gamma_{i,ic}^0 = \bar{\gamma}_{i,ic}^0 t$, assuming that the temperature and radiative properties are uniform throughout the cell. Internal luminescence $\gamma_{i,ic}^0$ and external luminescence $\gamma_{e,ic}^0$ of an isolated cell are plotted in Fig. 3 as references. The difference between these two quantities indicates the photon recycling level for an isolated cell due to reflection at its boundaries and reabsorption within the cell.

For the case of the Si emitter (Fig. 3(a)), external luminescence of propagating modes in vacuum ($0 < k_p < k_0$) varies with gap thickness. This is due to coherence effects arising from multiple

reflections in the vacuum gap [52,53]. External luminescence is up to 25% smaller or larger than the case of an isolated cell. For the Drude emitter (Fig. 3(b)), the impact from propagating modes in vacuum is reduced by a factor of approximately two compared to the case of an isolated cell since a significant portion of emission towards the emitter is reflected back to the cell and recycled. Thus, the corresponding external luminescence is dominated by emission towards the substrate.

The contribution to external luminescence by evanescent modes (frustrated and surface polariton modes) with $k_\rho > k_0$ is a strong function of the gap thickness, and becomes dominant at gap thicknesses smaller than 200 nm for both emitters. In the presence of the Si emitter, external luminescence increases (photon recycling decreases) by factors of 1.1 and 9.1 with respect to the far-field value at gap thicknesses of 1000 nm and 10 nm, respectively. In the limit that $d \rightarrow 0$, the cell external luminescence saturates since it is limited by modes with parallel wavevector $k_\rho < \text{Re}(m_{Si})k_0$. The Drude emitter allows tunneling all frustrated modes (propagating in the cell with $k_0 < k_\rho < \text{Re}(m_c)k_0$) dominating external luminescence between gap thicknesses of approximately 200 nm down to 50 nm. For gap thicknesses smaller than 50 nm, surface polariton modes in the cell with $k_\rho > \text{Re}(m_c)k_0$ dominate external luminescence. This change of dominant mode is caused by a shift in the dispersion relation at the emitter-vacuum interface due to the presence of the cell when the gap thickness is smaller than 70 nm. This shift was explained in Refs. [20,26] and reduces the contribution from modes $k_0 < k_\rho < \text{Re}(m_c)k_0$ and increases that from modes with parallel wavevectors exceeding $\text{Re}(m_c)k_0$. In the limit that $d \rightarrow 0$, external luminescence does not saturate but rather diverges since the limiting mode is characterized by a wavevector inversely proportional to the gap size ($k_\rho \approx 1/d$). At gap thicknesses of 10 nm and 1000 nm, the cell external luminescence respectively increases by a factor of 22.6 and remains

unchanged with respect to the far-field value. Clearly, while near-field TPV devices have the benefit of increasing radiation absorption by the cell due to tunneling of evanescent modes, the cell external luminescence is also substantially enhanced. The external luminescence enhancement is due to a drop in photon recycling, caused by the leakage towards the emitter of frustrated modes, and the intensification of spontaneous emission when the emitter supports surface polaritons modes.

The volumetric contribution by each discrete layer to external luminescence [(photons)/(cm³ s)] is plotted in Fig. 4 as a function of cell depth for the Si and Drude emitters and for gap and cell thicknesses of $d = 10$ nm and $t = 10$ μ m. This quantity is derived from Eq. (6) as:

$$\bar{\gamma}_e^0(d, \Delta z_j) = \frac{1}{\Delta z_j} \int_{\omega_g}^{\infty} \frac{1}{\exp[\hbar\omega / k_b T_c]} \left[\Phi_{c-e}(\omega, d, \Delta z_j) + \Phi_{c-s}(\omega, d, \Delta z_j) \right] \quad (9)$$

The volumetric internal luminescence of an isolated cell, $\bar{\gamma}_{i,ic}^0$, and the local volumetric contribution to external luminescence of an isolated cell, $\bar{\gamma}_{e,ic}^0$, are also plotted in Fig. 4. The former is uniform within the cell and the latter is symmetric with respect to the center of the cell. In the presence of an emitter, this symmetry is broken because of the addition of evanescent modes to external luminescence towards the emitter. The spatial distribution is a strong function of the emitter type. Local contributions to external luminescence are largest everywhere in the presence of the Si emitter except near the front surface of the cell (i.e., $z = 0$). Surface polaritons supported by the Drude emitter greatly enhance the cell local density of photon modes near $z = 0$. This is because the penetration depth in the cell of surface polariton modes dominating radiative transfer is approximately equal to the gap size d [49]. Near the cell front surface, the contribution to external luminescence with the Drude emitter even exceeds the internal luminescence of an

isolated cell by over an order of magnitude. The internal luminescence of an isolated cell, which does not account for the impact on spontaneous emission of surface polariton modes supported by the Drude emitter [20], is clearly invalid.

The external luminescence γ_e^0 dependence on cell thickness is shown in Fig. 5 for the Si and Drude emitters and for a gap thickness of $d = 10$ nm. The curves are compared against internal luminescence of an isolated cell $\gamma_{i,ic}^0$. Regardless of cell thickness, external luminescence with the Si emitter is smaller than internal luminescence because of photon recycling. The same is observed with the Drude emitter down to a cell thickness of 0.46 μm . As the cell thickness decreases, an increasing portion of its volume is affected by the presence of the Drude emitter. This implies that a larger portion of the cell can spontaneously emit modes with parallel wavevector exceeding $\text{Re}(m_c)k_0$ that are not taken into account in the internal luminescence model. In the limit that the cell thickness is comparable to the penetration depth of surface polaritons, which is approximately equal to the gap thickness, the density of modes of the entire cell is modified by the presence of the Drude emitter. For a 100-nm-thick cell, the external luminescence in the presence of the Drude emitter exceeds the internal luminescence of an isolated cell by nearly a factor of three. This means that spontaneous emission, and therefore radiative lifetime, can be greatly modified by the presence of an emitter supporting surface polariton modes, especially if the cell thickness is comparable to the vacuum gap thickness.

An alternative approach to account for radiative recombination in TPV devices involves the use of a spatially uniform radiative lifetime τ_{rad} [s] [20,22,26,28,30,32]. In low injection conditions, radiative lifetime of an isolated cell can be defined by $\tau_{rad} = 1/BN$, where N [carriers/cm³] is the doping concentration and B [(photons)cm³/s] is the radiative recombination coefficient. This

coefficient is related to internal luminescence of an isolated cell via the relation $B = \bar{\gamma}_{i,ic}^0 / n_i^2$, where n_i [carriers/cm³] is the intrinsic carrier concentration [36,54]. This approach assumes that all photons emitted are lost without any photon recycling. Also, any increase in available modes beyond $\text{Re}(m_c)k_0$ due to the presence of the Drude emitter is neglected. Near-field effects on photon recycling and spontaneous emission are therefore neglected in this approach.

In certain previous near-field TPV analyses, radiative recombination was implicitly assumed to be uniform within the cell via the radiative lifetime τ_{rad} while photon recycling was approximated using a photon recycling factor ϕ of 10 [22,26,28,32]. Such a factor is somehow arbitrary and neglects the aforementioned near-field impacts on photon recycling and spontaneous emission. A consistent photon recycling factor would need to be dependent on the emitter type as well as the cell and gap thicknesses (see Figs. 3 and 5). Therefore, it is clear that modeling radiative recombination with a spatially uniform radiative lifetime τ_{rad} corrected by a spatially uniform photon recycling factor ϕ should be avoided in near-field TPV performance prediction. Instead, a full radiation model, i.e. fluctuational electrodynamics with the generalized Planck function, should be used.

The impact of external luminescence enhancement in the near field on TPV performance is analyzed next when considering non-radiative recombination mechanisms.

IV. IMPACT OF EXTERNAL LUMINESCENCE ON NEAR-FIELD TPV PERFORMANCE

Assuming low injection conditions, non-radiative bulk Auger and Shockley-Read-Hall (SRH) recombination mechanisms are added to Eq. (1) as follows [29,36]:

$$\begin{aligned}
J(d, V) &= q \left[\gamma_a(d) - \gamma_e(d, V) - U_{Aug}(V) - U_{SRH}(V) \right] \\
&= q \left[\gamma_a(d) - \left(\gamma_e^0(d) - U_{Aug}^0 - U_{SRH}^0 \right) \exp \left(\frac{qV}{k_b T} \right) \right]
\end{aligned} \tag{10}$$

Auger and SRH equilibrium recombination rates are calculated as [55,56]:

$$U_{Aug}^0 = CN n_i^2 t \tag{11}$$

$$U_{SRH}^0 = \frac{n_i^2 t}{\tau_{SRH} N} \tag{12}$$

where C is the Auger recombination coefficient taking a value of $5 \times 10^{-30} \text{ cm}^6 \text{s}^{-1}$ for GaSb [57], N is the doping concentration fixed at 10^{18} cm^{-3} and τ_{SRH} is the lifetime associated with SRH recombination which is assumed to be 10 ns [57]. The intrinsic carrier concentration n_i of GaSb is taken as $1.5 \times 10^{12} \text{ cm}^{-3}$ at 300 K [57] and the cell thickness t is 10 μm . All results shown in this section are for the case of a Si emitter, since the conclusions are the same for the Drude emitter. Equivalent results for the Drude emitter are provided as Supplemental Material [58].

The impact of external luminescence on the cell J - V characteristic is analyzed first. The cell external luminescence has a component toward the emitter and a component toward the substrate. External luminescence towards the substrate can be minimized using efficient reflectors [59]. It follows that an external luminescence efficiency defined as:

$$\eta_{ext}(d) = \frac{\gamma_{e,c-e}^0(d)}{\gamma_e^0(d) + U_{Aug}^0 + U_{Aug}^0} \tag{13}$$

where only external luminescence toward the emitter $\gamma_{e,c-e}^0$ is accounted for in the numerator reflects solely the impact of the presence of the emitter on the J - V characteristic. Indeed, Eq. (10) can be reformulated as:

$$J(d, V) = q \left[\gamma_a(d) - \frac{\gamma_{e,c-e}^0(d)}{\eta_{ext}(d)} \exp\left(\frac{qV}{k_b T}\right) \right] \quad (14)$$

and the voltage at open circuit ($J = 0$) can thus be written as [59,60]:

$$V_{oc}(d) = \frac{k_b T}{q} \ln \left(\frac{\gamma_a(d)}{\gamma_{e,c-e}^0(d)} \right) - \frac{k_b T}{q} |\ln[\eta_{ext}(d)]| = V_{oc,ideal}(d) - \frac{k_b T}{q} |\ln[\eta_{ext}(d)]| \quad (15)$$

where $V_{oc,ideal}$ is the open-circuit voltage in the ideal case of the radiative limit with no cell external luminescence towards the substrate. Due to the reciprocity of radiative transfer between the emitter and the cell, γ_a and $\gamma_{e,c-e}^0$ have similar behaviors as a function of the gap thickness d causing $V_{oc,ideal}$ to be relatively independent of d . It follows that the dependence of open-circuit voltage on gap thickness is governed by the variations of the external luminescence efficiency η_{ext} . Since $\eta_{ext} \leq 1$, Eq. (15) is written using the absolute value of its natural logarithm to emphasize that the open-circuit voltage in real conditions is effectively smaller than that of the ideal case.

External luminescence efficiency and open-circuit voltage are plotted as a function of gap thickness for different cell conditions in Fig. 6. In the radiative limit, an external luminescence efficiency of 0.5 corresponds to equal emission leaving both sides of the cell. Therefore, external luminescence towards the Si emitter when $d = 1000$ nm is slightly affected by coherence effects of reflected propagating modes in the vacuum gap since $\eta_{ext} = 0.51$ and evanescent modes have a

negligible contribution. As the gap thickness decreases below 1000 nm, external luminescence towards the emitter becomes dominant due to tunneling of evanescent modes, such that external luminescence efficiency approaches unity and the open-circuit voltage approaches the ideal case. For a gap thickness of 10 nm, the open-circuit voltage enhancement compared to that in the far field is only 1.04 in the radiative limit, since the increase in external luminescence efficiency is only a factor of 2.09. This is because $\eta_{ext} = 0.45$ in the far field limiting the potential enhancement factor to approximately two.

The far-field external luminescence efficiencies are $\eta_{ext} = 5.2 \times 10^{-2}$ and 2.8×10^{-3} , respectively, when intrinsic radiative and Auger, and when all bulk recombination processes are accounted for. This allows for significant near-field enhancement in the external luminescence efficiency and, in turn, the open-circuit voltage when non-radiative recombination mechanisms are considered. The external luminescence efficiency enhancements at $d = 10$ nm due to near-field effects are 9.84 and 18.14 leading to open-circuit voltage enhancements of 1.15 and 1.23 when intrinsic radiative and Auger, and when all bulk recombination mechanisms are considered. This impact is shown in Fig. 7, where J - V characteristics for the ideal case of the radiative limit with no external luminescence towards the substrate and the case when all bulk recombination is considered are plotted. The open-circuit voltage offset, $(k_b T / q) \ln [\eta_{ext}(d)]$ in Eq. (15), with respect to the ideal open-circuit voltage is much smaller at $d = 10$ nm than in the far field when all bulk recombination mechanisms are considered. Therefore, while the near-field enhancement of absorption is identical in the two cases, the near-field enhancement of open-circuit voltage is more beneficial to the cell subject to non-radiative recombination.

The impact of gap thickness on power density at the maximum power point ($P = \max(JV)$) for the Si emitter and a 10- μm -thick cell is shown in Fig. 8. The power enhancement when $d = 10$ nm with respect to the far field case, P/P_{FF} , is 24.37 when considering all bulk recombination processes compared to 22.30 and 19.85 when intrinsic radiative and Auger and when only radiative recombination mechanisms are considered. The larger power enhancement when non-radiative recombination is significant is attributed to the larger enhancement in open-circuit voltage. It is concluded that TPV performance enhancement in the near field is more substantial when the cell exhibits significant non-radiative recombination. While high-quality cells always produce more power, the potential performance enhancement as the gap thickness decreases is larger for low quality cells due to the external luminescence enhancement caused by near-field effects.

Near-field performance enhancements at a gap thickness of 10 nm with respect to far-field conditions are summarized in Table I for the Si and Drude emitters. For the case of a Drude emitter, similar trends to that of the Si emitter are observed. The reason the near-field enhancement factors are significantly larger is because the Drude emitter is highly reflective in the far field, thus leading to an extremely small far-field external luminescence efficiency of 1.3×10^{-4} when considering all bulk recombination mechanisms.

V. CONCLUSIONS

The near-field impacts on photon recycling and spontaneous emission rate in TPV devices were investigated. This was accomplished by analyzing the cell external luminescence, calculated via fluctuational electrodynamics, in a TPV device consisting of either an intrinsic Si or a Drude emitter and a GaSb cell. Enhanced near-field external luminescence is due to an increase in the

available photon modes leading to a drop in photon recycling. The analysis showed that for gap thicknesses between the emitter and the cell less than 200 nm, evanescent modes, not contributing in far-field TPVs, dominate external luminescence for both emitter types. The enhancement of external luminescence in the near field with the Si emitter is caused by tunneling of modes propagating in the cell that otherwise fully contribute to photon recycling in far-field TPVs. The Drude emitter supporting surface polariton modes modifies the local density of photon modes in the cell, and thus leads to an increase of the cell spontaneous emission rate. This results in an additional channel for near-field external luminescence that allows tunneling of photon modes well beyond those propagating in the cell. For gap thicknesses on the order of a few tens of nanometers, the cell near-field external luminescence with a Drude emitter can even exceed the internal luminescence of an isolated cell. For a given cell material, the impact of radiative recombination must account for the emitter type as well as the gap and cell thicknesses, which cannot be captured with a spatially uniform radiative lifetime corrected by a photon recycling factor. Finally, the impact of external luminescence on near-field TPV performance was investigated when accounting for bulk non-radiative recombination processes. The results showed that the enhancement of external luminescence in the near field, causing the cell external luminescence efficiency to increase as the gap thickness decreases, has a positive impact on the open-circuit voltage and power density. Near-field TPV performance enhancement is the largest when all non-radiative bulk recombination processes are accounted for, thus suggesting that lower quality PV cells benefit more from the near-field effects of thermal radiation than high-quality cells approaching the radiative limit.

ACKNOWLEDGMENTS

This work was sponsored by the National Science Foundation under Grant No. CBET-1253577.

Rodolphe Vaillon acknowledges the financial support from the College of Engineering at the University of Utah (W.W. Clyde Visiting Chair award).

APPENDIX: TRANSMISSION FACTORS

The spectral, gap-dependent transmission factors needed to calculate the above bandgap photon flux absorbed by the cell and the above bandgap photon emission lost to the surroundings (i.e., cell external luminescence) are derived using dyadic Green's functions for layered media [61]. These dyadic Green's functions are spatial transfer functions relating the electric and magnetic fields observed at location z generated by a mode with parallel wavevector k_ρ and angular frequency ω to a source point located at z' . The transmission factor relating the entire volume of the emitter to a discrete layer of thickness Δz_j within the cell delimited by the boundaries z_j and z_{j+1} is given by [46]:

$$\Phi_{e-c}(\omega, d, \Delta z_j) = \frac{k_0^2}{2\pi^2} \operatorname{Re} \left\{ i \operatorname{Im}(\epsilon_e) \int_0^\infty \frac{k_\rho dk_\rho}{\operatorname{Im}(k_{ze})} \left[\begin{array}{c} g_{ec\rho\alpha}^E(k_\rho, z_j, \omega, d) g_{ec\theta\alpha}^{H*}(k_\rho, z_j, \omega, d) \\ -g_{ec\theta\alpha}^E(k_\rho, z_j, \omega, d) g_{ec\rho\alpha}^{H*}(k_\rho, z_j, \omega, d) \\ -g_{ec\rho\alpha}^E(k_\rho, z_{j+1}, \omega, d) g_{ec\theta\alpha}^{H*}(k_\rho, z_{j+1}, \omega, d) \\ -g_{ec\theta\alpha}^E(k_\rho, z_{j+1}, \omega, d) g_{ec\rho\alpha}^{H*}(k_\rho, z_{j+1}, \omega, d) \end{array} \right] \right\} \quad (A1)$$

where the g terms are the Weyl (plane wave) components of the dyadic Green's functions, the subscript α involves a summation over the three orthogonal components, E and H refer to electric and magnetic fields and $*$ is the complex conjugate. In Eq. (A1), an integration is performed over all possible photon modes k_ρ . The transmission factor relating a discrete layer Δz_j within the cell to the entire volume of the emitter Φ_{c-e} is equal to Φ_{e-c} due to the reciprocity of the dyadic Green's function.

The transmission factor relating a discrete layer Δz_j within the cell to the entire volume of the substrate is given by [46]:

$$\Phi_{c-s}(\omega, d, \Delta z_j) = \frac{k_0^2}{2\pi^2} \operatorname{Re} \left\{ i \operatorname{Im}(\epsilon_s) \int_0^{k_0} \frac{k_\rho dk_\rho}{\operatorname{Im}(k_{zs})} \begin{bmatrix} g_{sc\rho\alpha}^E(k_\rho, z_{j+1}, \omega, d) g_{sc\theta\alpha}^{H*}(k_\rho, z_{j+1}, \omega, d) \\ -g_{sc\theta\alpha}^E(k_\rho, z_{j+1}, \omega, d) g_{sc\rho\alpha}^{H*}(k_\rho, z_{j+1}, \omega, d) \\ -g_{sc\rho\alpha}^E(k_\rho, z_j, \omega, d) g_{sc\theta\alpha}^{H*}(k_\rho, z_j, \omega, d) \\ -g_{sc\theta\alpha}^E(k_\rho, z_j, \omega, d) g_{sc\rho\alpha}^{H*}(k_\rho, z_j, \omega, d) \end{bmatrix} \right\} \quad (\text{A2})$$

where the summation over the photon modes k_ρ is limited to propagating modes in the substrate k_0 .

Explicit expressions for the Weyl components of the dyadic Green's functions needed to compute Eqs. (A1) and (A2) are provided in Ref. [46].

REFERENCES

- [1] T. J. Coutts, Sol. Energy Mater. Sol. Cells **66**, 443 (2001).
- [2] T. Bauer, *Thermophotovoltaics: Basic Principles and Critical Aspects of System Design* (Springer, Berlin, 2011).
- [3] R. M. Swanson, P. IEEE **67**, 446 (1979).
- [4] F. Demichelis, E. Minetti-Mezzetti, Sol. Cells **1**, 395 (1980).
- [5] T. A. Butcher, J. S. Hammonds, E. Horne, B. Kamath, J. Carpenter and D. R. Woods, Appl. Energ. **88**, 1543 (2011).
- [6] D. Polder and M. Van Hove, Phys. Rev. B **4**, 3303 (1971).

- [7] J.-P. Mulet, K. Joulain, R. Carminati and J.-J. Greffet, *Microscale Therm. Eng.* **6**, 209 (2002).
- [8] L. Hu, A. Narayanaswamy, *Appl. Phys. Lett.* **92**, 133106 (2008).
- [9] E. Rousseau, A. Siria, G. Jourdan, S. Volz, F. Comin, J. Chevrier and J.-J. Greffet, *Nat. Photonics* **3**, 514 (2009).
- [10] S. Shen, A. Narayanaswamy and G. Chen, *Nano Lett.* **9**, 2909 (2009).
- [11] R. S. Ottens, V. Quetschke, S. Wise, A. A. Alemi, R. Lundock, G. Mueller, D. H. Reitze, D. B. Tanner and B. F. Whiting, *Phys. Rev. Lett.* **107**, 014301 (2011).
- [12] T. Ijiro and N. Yamada, *Appl. Phys. Lett.* **106**, 023103 (2015).
- [13] K. Ito, A. Miura, H. Iizuka and H. Toshiyoshi, *Appl. Phys. Lett.* **106**, 083504 (2015).
- [14] M. Lim, S. S. Lee and B. J. Lee, *Phys. Rev. B* **91**, 195136 (2015).
- [15] B. Song, D. Thompson, A. Fiorino, Y. Ganjeh, P. Reddy, E. Meyhofer, *Nat. Nanotechnol.* **11**, 509 (2016).
- [16] M.P. Bernardi, D. Milovich and M. Francoeur, *Nat. Communications* **7**, 12900 (2016).
- [17] R. S. DiMatteo, P. Greiff, S. L. Finberg, K. A. Young-Waithe, H. K. H. Choy, M. M. Masaki and C. G. Fonstad, *Appl. Phys. Lett.* **79**, 1894 (2001).
- [18] M. D. Whale and E. G. Cravalho, *IEEE T. Energy Conver.* **17**, 130 (2002).
- [19] A. Narayanaswamy, and G. Chen, *Appl. Phys. Lett.* **82**, 3544 (2003).
- [20] M. Laroche, R. Carminati and J.-J. Greffet, *J. Appl. Phys.* **100**, 063704 (2006).

- [21] K. Park, S. Basu, W. P. King and Z. M. Zhang, *J. Quant. Spectrosc. Radiat. Transfer* **109**, 305 (2008).
- [22] M. Francoeur, R. Vaillon and M. P. Mengüç, *IEEE T. Energy Conver.* **26**, 686 (2011).
- [23] O. Ilic, M. Jablan, J. D. Joannopoulos, I. Celanović and M. Soljačić, *Opt. Express* **20**, A366 (2012).
- [24] R. Messina and P. Ben-Abdallah, *Sci. Rep.* **3**, 1383 (2013).
- [25] V. B. Svetovoy and G. Palasantzas, *Phys. Rev. Appl.* **2**, 034006 (2014).
- [26] M. P. Bernardi, O. Dupré, E. Blandre, P.-O. Chapuis, R. Vaillon and M. Francoeur, *Sci. Rep.* **5**, 11626 (2015).
- [27] M. Lim, S. Jin, S. S. Lee and B. J. Lee, *Opt. Express* **23**, A240 (2015).
- [28] M. Elzouka and S. Ndao, Towards a near-field concentrated solar thermophovoltaic microsystem: part I – modeling, *Sol. Energy*, In Press (2015).
- [29] K. Chen, P. Santhanam and S. Fan, *Appl. Phys. Lett.* **107**, 091106 (2015).
- [30] J. K. Tong, W.-C. Hsu, Y. Huang, S. V. Boriskina and G. Chen, *Sci. Rep.* **5**, 10661 (2015).
- [31] A. Karalis and J. D. Joannopoulos, *Sci. Rep.* **6**, 28472 (2016).
- [32] J. Z.-J. Lau, V. N.-S. Bong and B. T. Wong, *J. Quant. Spectrosc. Radiat. Transfer* **171**, 39 (2016).
- [33] S. V. Boriskina, M. A. Green, K. Catchpole, E. Yablonovitch, M. C. Beard, Y. Okada, S. Lany, T. Gershon, A. Zakutayev, M. H. Tahersima, V. J. Sorger, M. J. Naughton, K.

- Kempa, M. Dagenais, Y. Yao, L. Xu, X. Sheng, N. D. Bronstein, J. A. Rogers, A. P. Alivisatos, R. G. Nuzzo, J. M. Gordon, D. M. Wu, M. D. Wisser, A. Salleo, J. Dionne, P. Bermel, J.-J. Greffet, I. Celanovic, M. Soljacic, A. Manor, C. Rotschild, A. Raman, L. Zhu, S. Fan and G. Chen, *J. Opt.* **18**, 073004 (2016).
- [34] K. Okamoto, I. Niki, A. Shvartser, Y. Narukawa, T. Mukai and A. Scherer, *Nat. Mater.* **3**, 601 (2004).
- [35] W. Shockley and H. J. Queisser, *J. Appl. Phys.* **32**, 510 (1961).
- [36] A. Marti, J. L. Balenzategui and R. F. Reyna, *J. Appl. Phys.* **82**, 4067 (1997).
- [37] R. J. Kumar, J. M. Borrego, P.S. Dutta and R. J. Gutmann, *J. Appl. Phys.* **97**, 023530 (2005).
- [38] S. Adachi, *J. Appl. Phys.* **66**, 6030 (1989).
- [39] E. D. Palik, *Handbook of Optical Constants of Solids* (Academic Press, San Diego, 1998).
- [40] S. A. Maier, *Plasmonics: Fundamentals and Applications* (Springer, New York, 2007).
- [41] M. A. Green, *Third Generation Photovoltaics: Advanced Solar Energy Conversion* (Springer, Germany, 2003).
- [42] S. M. Rytov, Y. A. Kravtsov and V. I. Tatarskii, *Principles of Statistical Radiophysics 3: Elements of Random Fields* (Springer, New York, 1989).

- [43] K. Kim, B. Song, V. Fernández-Hurtado, W. Lee, W. Jeong, L. Cui, D. Thompson, J. Feist, M. T. H. Reid, F. J. Garcia-Vidal, J. C. Cuevas, E. Meyhofer and P. Reddy, *Nature* **528**, 387 (2015).
- [44] V. Chiloyan, J. Garg, K. Esfarjani and G. Chen, *Nat. Communications* **6**, 6755 (2015).
- [45] P. Würfel, *J. Phys. C. Solid State* **15**, 3967 (1982).
- [46] M. Francoeur, M. P. Mengüç and R. Vaillon, *J. Quant. Spectrosc. Radiat. Transfer* **110**, 2002 (2009).
- [47] L. C. Hirst and N. J. Ekins-Daukes, *Prog. Photovoltaics* **19**, 286 (2010).
- [48] S.-A. Biehs, E. Rousseau and J.-J. Greffet, *Phys. Rev. Lett.* **105**, 234301 (2010).
- [49] M. Francoeur, M. P. Mengüç and R. Vaillon, *Phys. Rev. B* **84**, 075436 (2011).
- [50] W. van Roosbroeck and W. Shockley, *Phys. Rev.* **94**, 1558 (1954).
- [51] T. Trupke, M. A. Green, P. Würfel, P. P. Altermatt, A. Wang, J. Zhao and R. Corkish, *J. Appl. Phys.* **94**, 4930 (2003).
- [52] Y. Tsurimaki, P.-O. Chapuis, J. Okajima, A. Komiya, S. Maruyama and R. Vaillon, *J. Quant. Spectrosc. Radiat. Transfer* **187**, 310 (2017).
- [53] A. Narayanaswamy and J. Mayo, *J. Quant. Spectrosc. Radiat. Transfer* **184**, 254 (2016).
- [54] P. Würfel, *Physics of Solar Cells: From Basic Principles to Advanced Concepts* (Wiley-VCH, 2009).
- [55] M. A. Green, *IEEE T. Electron Dev.* **31**, 671 (1984).

- [56] A. Cuevas, Energy Procedia **55**, 53 (2014).
- [57] G. Stollwerck, O. V. Sulima and A. W. Bett, IEEE T. Electron Dev. **47**, 448 (2000).
- [58] See Supplemental Material at [URL will be inserted by publisher] for figures showing TPV performance with a Drude emitter: external luminescence efficiency as a function of gap thickness, *J-V* characteristics, and power density enhancement as a function of gap thickness.
- [59] O. D. Miller, E. Yablonovitch and S. R. Kurtz, IEEE Journal of Photovoltaics **2**, 303 (2012).
- [60] R. T. Ross, J. Chem. Phys. **46**, 4590 (1967).
- [61] J. E. Sipe, J. Opt. Soc. Am. B **4**, 481 (1987).

FIGURES

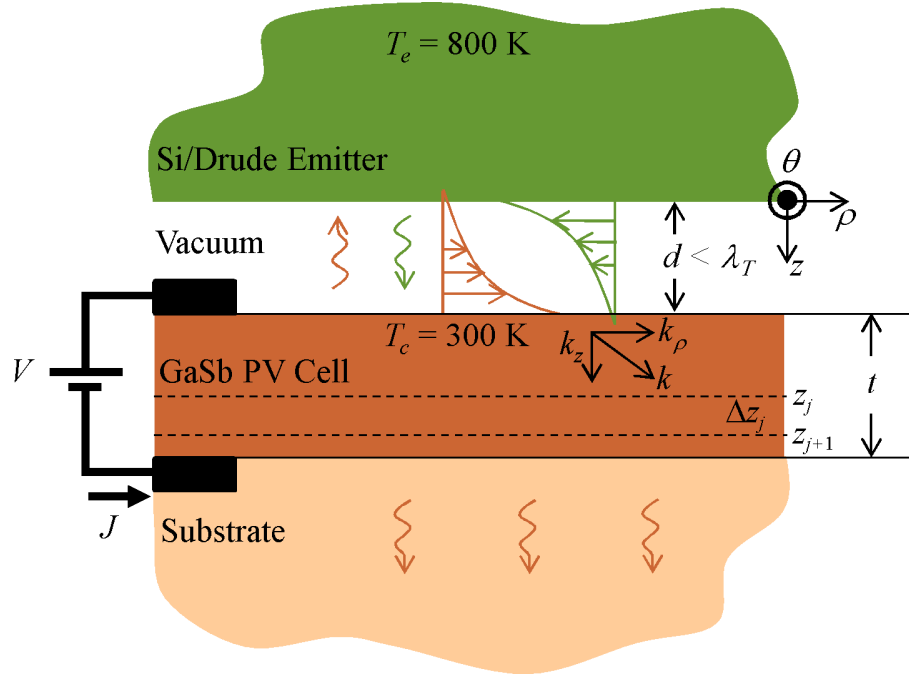


FIG. 1. (Color online) Schematic of a near-field TPV device showing contributions of propagating and evanescent modes to photon exchange. The emitter and PV cell, separated by a vacuum gap of thickness (d) smaller than the thermal wavelength (λ_T), are at constant and uniform temperatures of 800 K and 300 K, respectively.

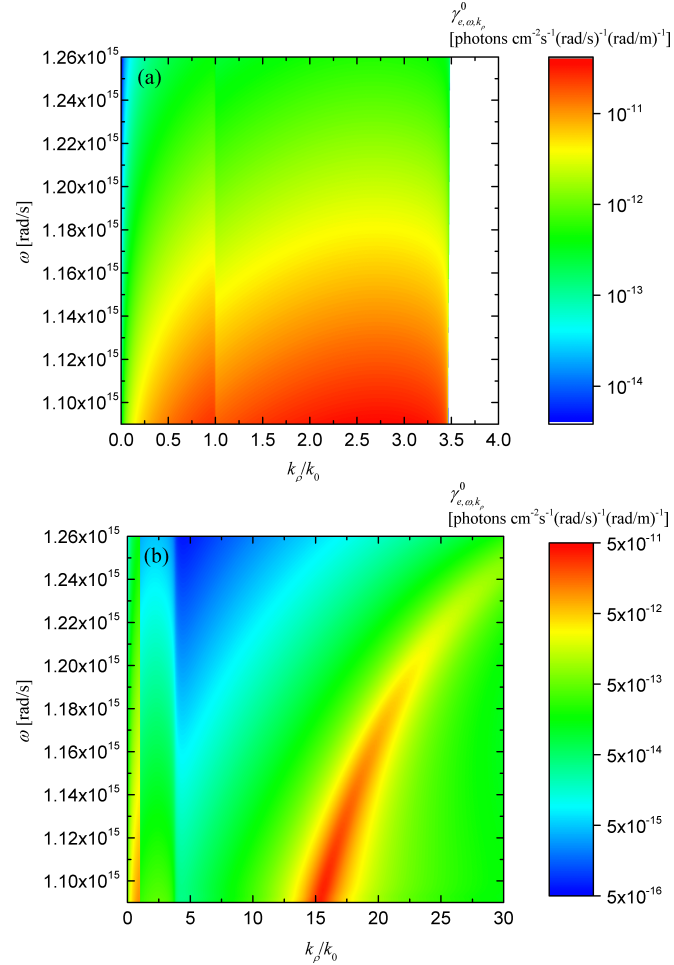


FIG. 2. (Color online) Cell external luminescence in chemical equilibrium ($\gamma_{e,\omega,k_\rho}^0$) as a function of angular frequency (ω) and normalized parallel wavevector (k_ρ/k_0) for $d = 10$ nm and $t = 10$ μm : (a) Si emitter. (b) Drude emitter.

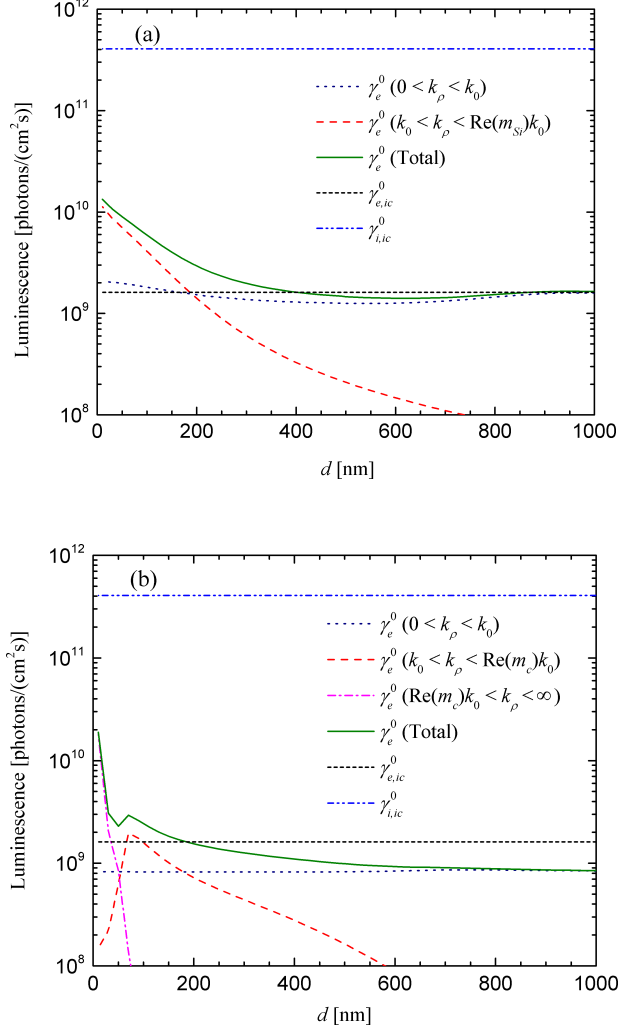


FIG. 3. (Color online) Cell external luminescence in chemical equilibrium (γ_e^0) as a function of the gap thickness (d) for $t = 10 \mu\text{m}$: (a) Si emitter. (b) Drude emitter. For comparison, internal luminescence ($\gamma_{i,ic}^0$) and external luminescence ($\gamma_{e,ic}^0$) of an isolated cell are also plotted.

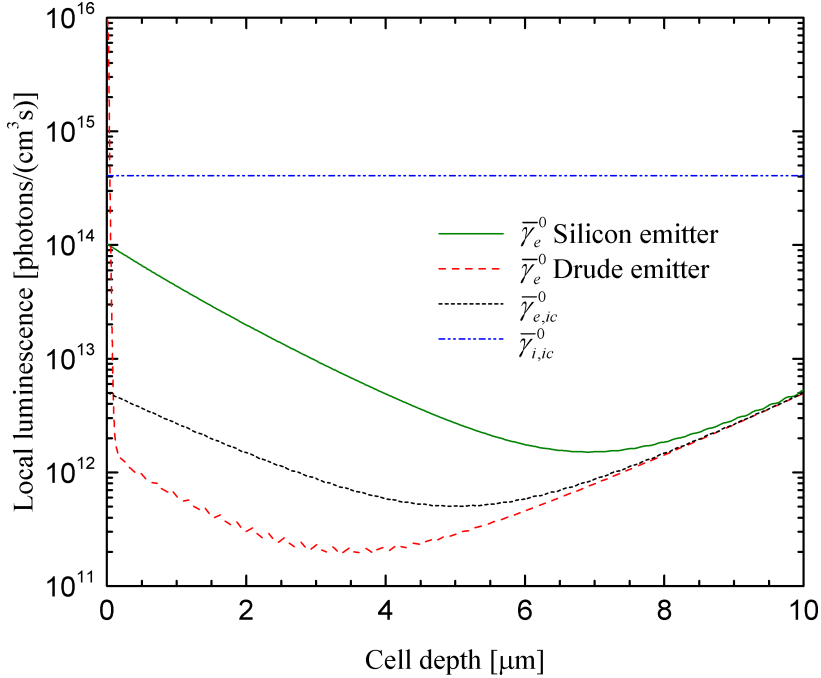


FIG. 4. (Color online) Local volumetric contribution to the cell external luminescence in chemical equilibrium ($\bar{\gamma}_e^0$) as a function of depth into the cell for $d = 10$ nm and $t = 10$ μm . For comparison, local volumetric internal luminescence in chemical equilibrium ($\bar{\gamma}_{i,ic}^0$) and local volumetric contribution to external luminescence of an isolated cell ($\bar{\gamma}_{e,ic}^0$) are plotted.

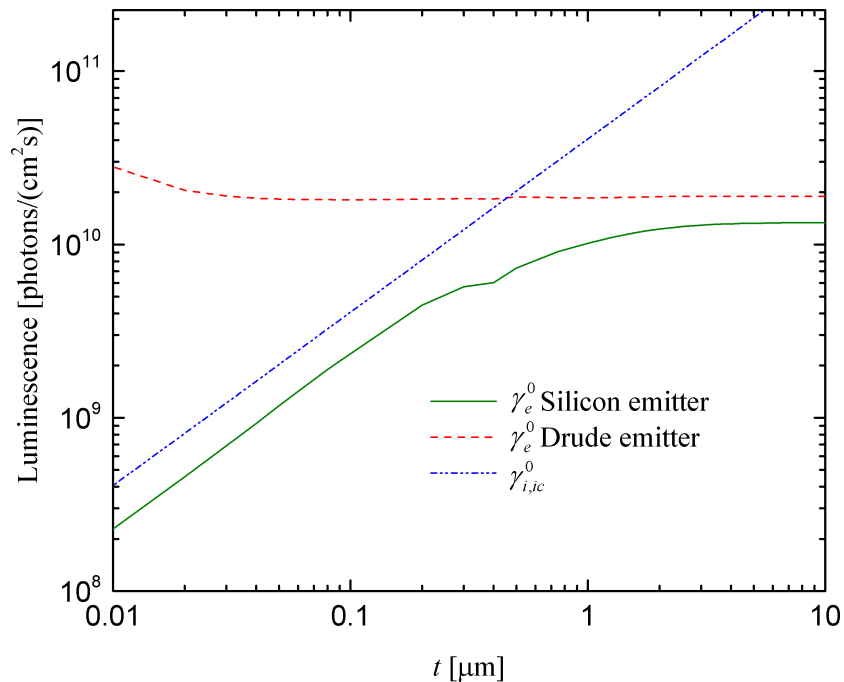


FIG. 5. (Color online) Cell external luminescence in chemical equilibrium (γ_e^0) as a function of the cell thickness (t) for $d = 10$ nm. For comparison, internal luminescence of an isolated cell ($\gamma_{i,ic}^0$) is plotted.

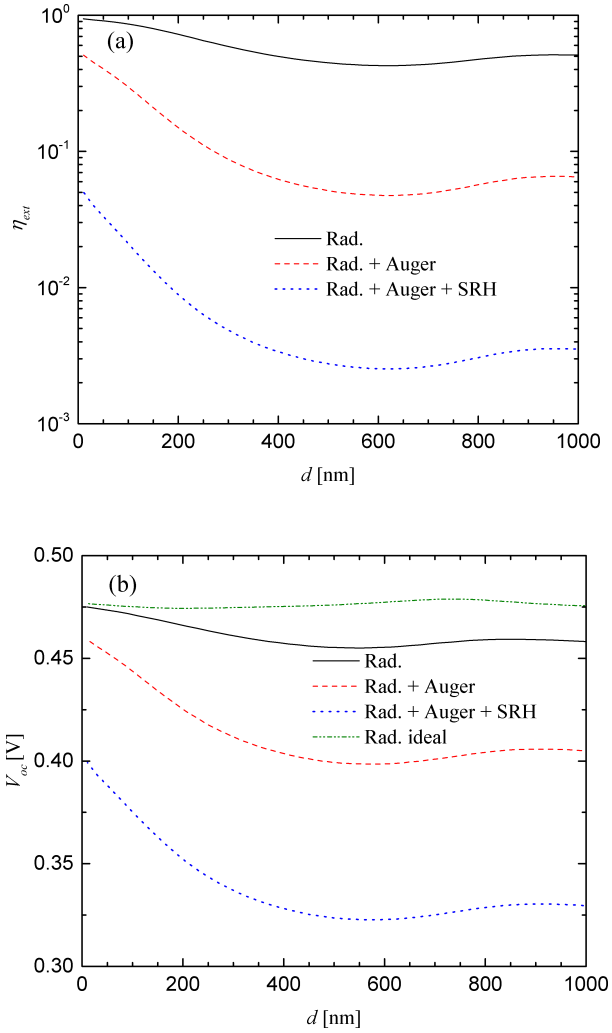


FIG. 6. (Color online) (a) Cell external luminescence efficiency (η_{ext}) and (b) open-circuit voltage (V_{oc}), as a function of the gap thickness (d) for the case of the Si emitter, when only radiative (Rad.), intrinsic (Rad. + Auger) and all (Rad. + Auger + SRH) recombination processes are considered. The open-circuit voltage in the ideal case of the radiative limit with no luminescence towards the substrate (Rad. ideal) is plotted in panel (b).

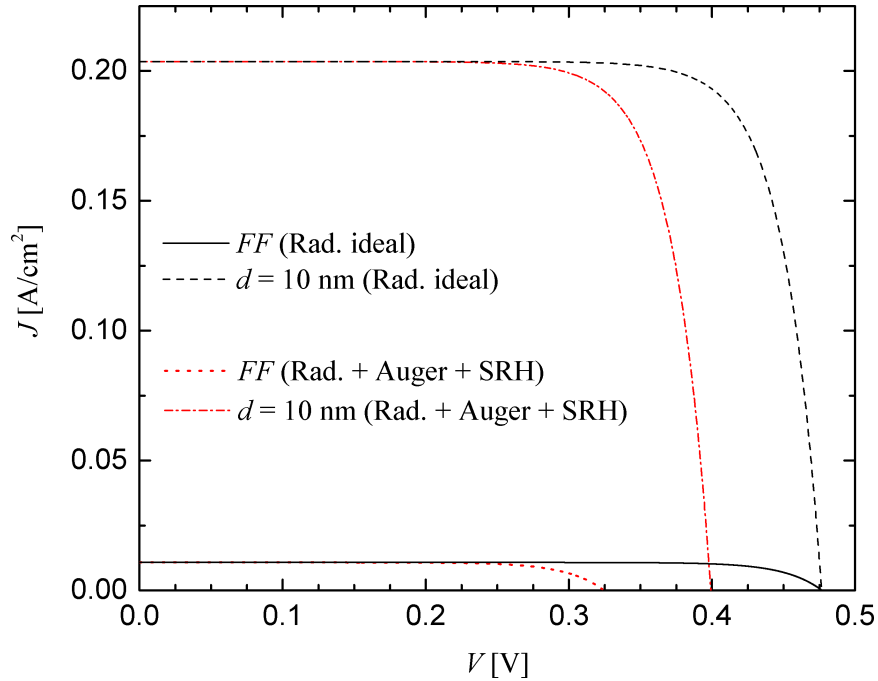


FIG. 7. (Color online) J - V characteristics for a gap thickness of 10 nm and in the far field (FF) for the Si emitter, in the ideal case of the radiative limit with no luminescence towards the substrate (Rad. ideal) and that with all (Rad. + Auger + SRH) recombination processes.

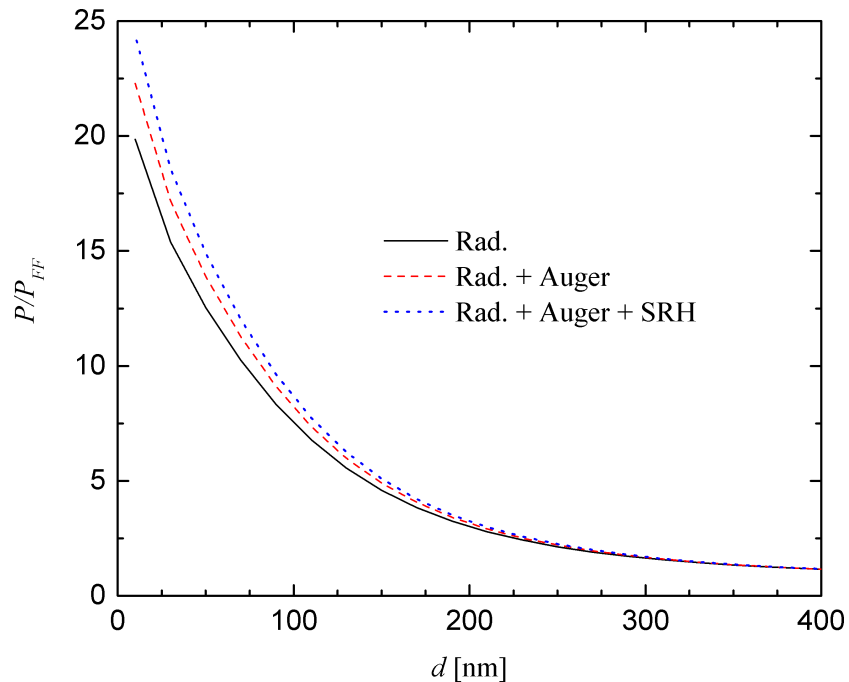


FIG. 8. (Color online) TPV power density enhancement (P/P_{FF}) as a function of the gap size (d) for $t = 10 \mu\text{m}$ for the case of the Si emitter, when only radiative (Rad.), intrinsic (Rad. + Auger) and all (Rad. + Auger + SRH) recombination processes are considered.

TABLE I. Near-field TPV performance enhancement (power density P , external luminescence efficiency η_{ext} , open-circuit voltage V_{oc}) at a gap thickness of 10 nm with respect to far-field (FF) conditions. Results are given when only radiative (Rad.), intrinsic (Rad. + Auger) and all (Rad. + Auger + SRH) recombination processes are considered.

Silicon emitter			
	Rad.	Rad. + Auger	Rad. + Auger + SRH
P/P_{FF}	19.85	22.30	24.37
$\eta_{ext}/\eta_{ext,FF}$	2.09	9.84	18.14
$V_{oc}/V_{oc,FF}$	1.04	1.15	1.23
Drude emitter			
	Rad.	Rad. + Auger	Rad. + Auger + SRH
P/P_{FF}	850.89	1046.94	1272.36
$\eta_{ext}/\eta_{ext,FF}$	26.83	242.45	562.10
$V_{oc}/V_{oc,FF}$	1.22	1.45	1.68

Supplemental Material for article “External luminescence and photon recycling in
near-field thermophotovoltaics”

John DeSutter^{*}, Rodolphe Vaillon^{**, *} and Mathieu Francoeur^{*,†}

^{*}*Radiative Energy Transfer Lab, Department of Mechanical Engineering, University of Utah,
Salt Lake City, UT 84112, USA*

^{**}*Univ Lyon, CNRS, INSA-Lyon, Université Claude Bernard Lyon 1, CETHIL UMR5008, F-
69621, Villeurbanne, France*

(Dated: December 6, 2016)

[†] Corresponding author. Tel.: +1 801 581 5721
Email address: mfrancoeur@mech.utah.edu

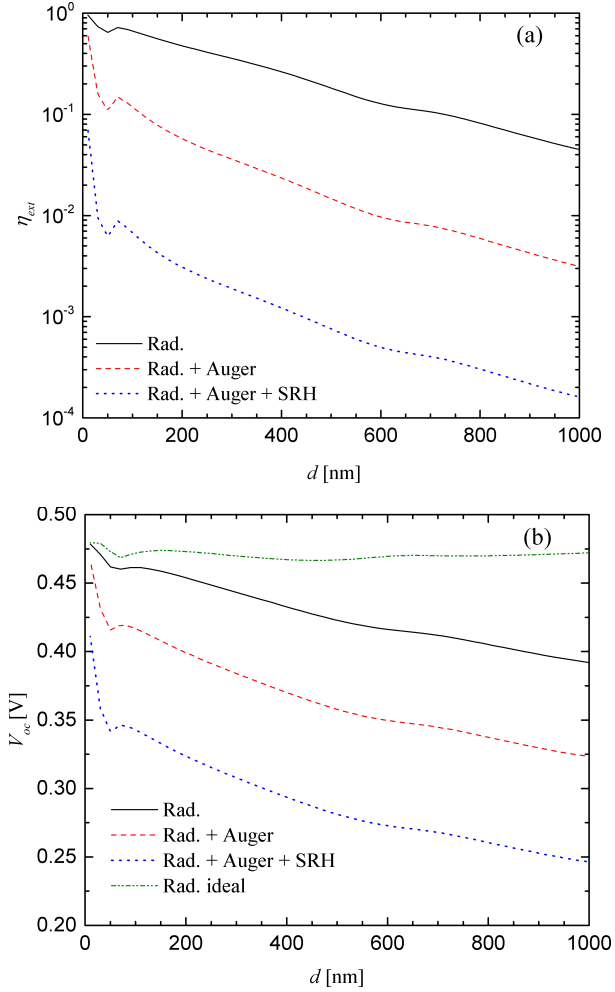


FIG. S1. (Color online) (a) Cell external luminescence efficiency (η_{ext}) and (b) open-circuit voltage (V_{oc}), as a function of the gap thickness (d) for the case of the Drude emitter, when only radiative (Rad.), intrinsic (Rad. + Auger) and all (Rad. + Auger + SRH) recombination processes are considered. The open-circuit voltage in the ideal case of the radiative limit with no luminescence towards the substrate (Rad. ideal) is plotted in panel (b).

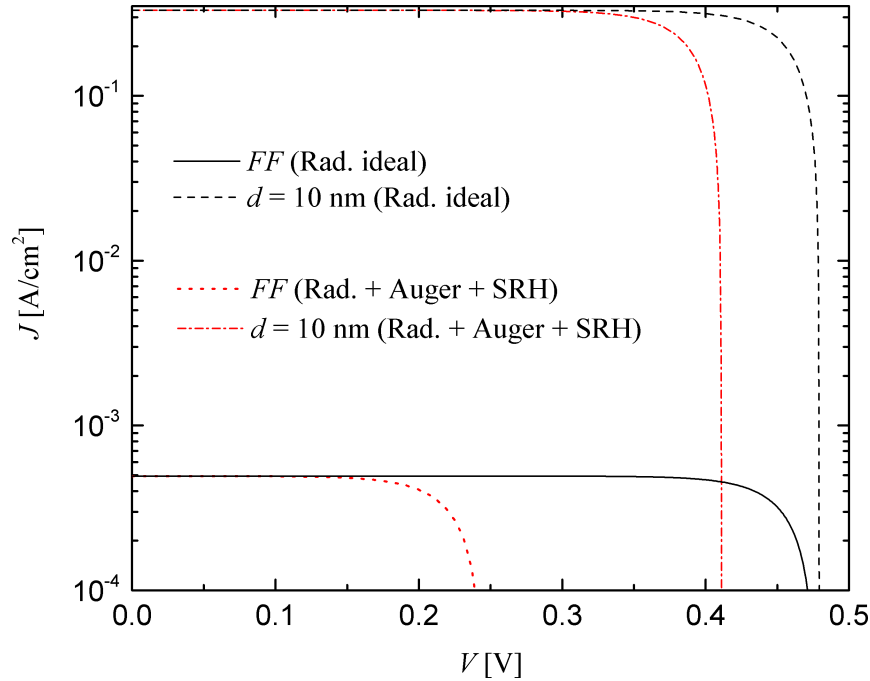


FIG. S2. (Color online) J - V characteristics for a gap thickness of 10 nm and in the far field (FF) for the Drude emitter, in the ideal case of the radiative limit with no luminescence towards the substrate (Rad. ideal) and that with all (Rad. + Auger + SRH) recombination processes.

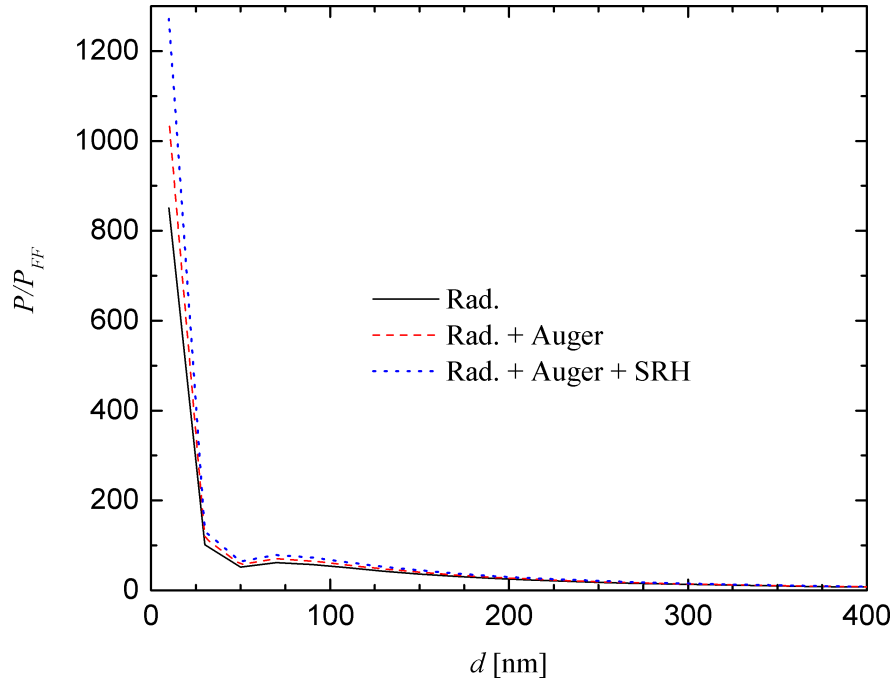


FIG. S3. (Color online) TPV power density enhancement (P/P_{FF}) as a function of the gap size (d) for $t = 10 \mu\text{m}$ for the case of the Drude emitter, when only radiative (Rad.), intrinsic (Rad. + Auger) and all (Rad. + Auger + SRH) recombination processes are considered.